

# SEMI-AUTOMATIC CORRECTION OF DIGITAL IMAGES OF FLAT OBJECTS

Antonio Luis Berberan  
Research Engineer, National Laboratory for Civil Engineering, Portugal  
[berberan@lnec.pt](mailto:berberan@lnec.pt)

CIPA, Task Group 2

**KEY WORDS:** photogrammetry, amateur camera, digital photography, single image and conservation

## ABSTRACT:

*A large number of important objects, which need to be surveyed, develop according to a mathematical surface, without significant relief. That fact allows the use of monoscopic photogrammetry instead of the stereoscopic approach, which is more demanding in terms of equipment and procedures as well as concepts and models, personnel training and skills. This paper describes an easy to use semi-automatic methodology that allows an easy, fast and inexpensive in-situ surveying of what might be considered as flat objects. An amateur camera with 1280x1024 CCD sensors, 6.8mmx6.8mm each, acquires the images and downloads it to a portable computer. The method uses robustified artificial vision techniques to read, semi-automatically, object-referenced points. The image is rectified in-situ in order to evaluate its quality. After rectification, the image has geometric quality and can be vectorised, in office, within half pixel image accuracy allowing object accuracy better than one centimetre, at 15 meters range, for this particular camera.*

## 1 INTRODUCTION

The main difficulty on using photogrammetric techniques for the vectorization of objects resides in the highly specialization involved both in terms of equipment and human resources. This paper summarises an easy-to-use monoscopic system, which has been implemented in a portable computer attached to an amateur digital camera. In a practical example, the system collects an image of what might be considered as a flat facade and provides, semi-automatically and *in-situ*, a rectified image of the object.

Because the facade is considered flat, stereoscopy is not used, i.e. no numerical model of the object relief is collected. On the other hand, the image, which is registered through a lens system, has not a uniform scale all over its area and can not be immediately used for metric purposes but the rectified image can be vectorized with geometric quality.

In order to improve the referred quality, the calibration parameters of the amateur camera have to be determined and used to resample the image, free of their effects. The calibration process implies the measurement of a relatively large number of image points. With digital or digitized photographs and using artificial vision techniques it is possible to measure automatically many reference points in an accurate, reliable and fast way in order to solve the previous two problems. Some leveling rods provide a reasonable amount of reference points.

Following the automatic measuring process, the interior (calibration) and exterior (spatial position of the center of the lens and attitude of the optical axis) parameters of the camera are determined and a new (resampled) image of the flat facade is obtained. This resampled image has uniform scale as if the camera lens was error free and the image plane, at the time of exposure, was parallel to the facade. The resampled raster image may be used for metric purposes as to vectorize facades, archeological mosaics, panels, stained glass windows and the like. Other mathematical surfaces can be handled as spherical domes, cylindrical walls, etc..

Pictures were taken with a Olympus Camedia C1400L with 1280x1024 CCD sensor elements whose size has been determined to be 6,8µm x 6,8µm. The lens system has seven elements and is of zoom type (focal distance varying between 9.2mm and 24mm). The image is compressed in JPG format.

## 2 IMAGE ACQUISITION

### 2.1 Image formation

From a geometric point of view the image results from a central projection of a three dimensional space into a two dimensional space. If that object can be considered as belonging to a mathematical continuous surface, than one single image is enough to reconstruct it, provided the whole object is in sight from the photographic station. Otherwise (there is relief in the object) a second image has to be taken from a different station in order to reconstruct a three dimensional model of the object. The lack of relief thus facilitates the task at end both in terms of the mathematical problem, specialized knowledge and skill of the operators, as well as software and hardware requirements.

### 2.2 Perturbations in image formation

One digital image represents geometric and radiometric information respectively expressed by the pixel position and by the radiometric level. Both types of information can be perturbed in what concerns the theoretical models that they are supposed to abide. The causes perturbing the radiometric information can be noise (thermal energy is understood as light), transfer inefficiency (the registered value is lower than the value gathered by the sensor) and the non-linearity of the sensor (the registered values are not proportional to the amount of light). These error sources are usually within acceptable limits and have no practical influence in the image formation.

As far as the geometric problem is concerned, lens systems have two types of deficiency which result in the light not propagating in a straight line as theoretically acceptable. One of these types of deficiency (lens are spherical and not revolution paraboloids) leads to the so-called radial distortion while the second type

(lack of alignment among the optical axes of the individual lenses of the system) leads to the so-called tangential distortion. The first is represented by a polynomial function of the radial distance  $r$  to the principal point:

$$dr = K_1 r^3 + K_2 r^5 + K_3 r^7 \quad \text{eq. (1)}$$

Two relations, one for each co-ordinate axis, model the tangential distortion:

$$\begin{aligned} d_x &= P_1 [r^2 + 2(x' - x_o)^2] + 2P_2 (x' - x_o)(y' - y_o) \\ d_y &= P_2 [r^2 + 2(y' - y_o)^2] + 2P_1 (x' - x_o)(y' - y_o) \end{aligned} \quad \text{eq. (2)}$$

where  $r$  is the radial distance between the image point, with image co-ordinates  $(x', y')$ , and the intersection, with image co-ordinates  $(x_o, y_o)$ , of the optical axis with the image plane.

### 3 MATHEMATICAL BACKGROUND

#### 3.1 Self-calibrating external orientation

External orientation is the determination of position of the lens centre (object co-ordinates  $X_F, Y_F, Z_F$ ) and its optical axis (angles  $w, f, k$  which refer the mentioned axis to the object reference system). The external orientation implies the measurement of image co-ordinates  $(x, y)$  of points with known object co-ordinates  $(X, Y, Z)$  and the use of a linearisation of the colinearity equations which relate the known quantities  $(x, y, X, Y, Z)$  of each observed point with the unknowns  $(X_F, Y_F, Z_F, w, f, k)$ . If, besides these unknowns, the calibration parameters  $K_1, K_2, K_3, P_1$  and  $P_2$  (generically represented as  $Dx$  e  $Dy$ ) are included in the functional model one says that a self-calibration is taking place, together with the external orientation. The observation of a set of points leads to a linearized, non-homogeneous and, if redundant, inconsistent system of equations expressed matricially as  $Ax=l$ .

The observed quantities are stochastic in nature. This fact is characterised by the diagonal matrix  $D = S^2 I$  where  $S^2$  is the variance of the observed quantities  $(x, y)$  and  $I$  is the identity matrix. This means that the observations are considered as not correlated and of the same precision. None of the assumptions occur in reality but one can seldom afford to model the observations with better fidelity. This simplification, of the probabilistic model, has no practical consequences in the quality of the results and eases significantly the processing time and mathematical elaboration of the problem. The solution,

$$\hat{x} = (A^t D^{-1} A)^{-1} x - A^t D^{-1} l, \quad \text{eq. (3)}$$

of the above referred equation system is determined using the robustified least square method [Berberan, 1996] and will provide the determination of the exterior and interior orientation parameters of the camera.

#### 3.2 Ill conditioning of the system of equations

The determination of a solution for  $Ax=l$  might (and probably will) be ill conditioned as a result of the overparametrisation caused by the introduction of the calibration parameters into the functional model. These parameters correlate among themselves and the exterior orientation ones. The referred correlation has to

be carefully analyzed. The problem has been addressed computing three quantities, namely :

- Statistical correlation ( $\rho$ ) between estimated parameters  $\hat{x}_i$  and  $\hat{x}_j$

$$r = \frac{S_{\hat{x}_i \hat{x}_j}}{S_{\hat{x}_i} S_{\hat{x}_j}}$$

- Measure of the determinability  $b_{ii}$  of the unknowns

$$b_{ii} = \left( I - ((diag(A^t D^{-1} A) \cdot diag(A^t D^{-1} A)^{-1})^{-1}) \right)_{ii}$$

- Test statistic  $t$ , a function of the  $m-1$  degrees of freedom and of  $\alpha$ , the confidence level

$$t_{m-1, \alpha/2} = \frac{\hat{x}_i}{S_{\hat{x}_i}}$$

The first quantity may vary between  $-1$  and  $1$ , representing  $0$  the orthogonalisation of the pertinent columns of  $A$  i.e. the independence of the parameters. Its absolute value should be kept under  $0.90$ . The second quantity will vary between  $0$  (matrix  $A^t D^{-1} A$  is diagonal) and  $1$  (matrix  $A^t D^{-1} A$  is singular) and should be kept under  $0.85$  [Kraus, 1997]. The third and last quantity refers to the *t-Student* distribution which is used in testing the null hypothesis  $H_0$ : “parameter  $\hat{x}_i$  is not significant”

against the alternative hypothesis  $H_a$ : “parameter  $\hat{x}_i$  is significant”. A decision should be taken, after skilled analysis of the three values, as to include or not each one of the interior parameters what can be done using the unified least squares approach [Mikhail, 1976].

### 4 AUTOMATIC MEASUREMENT

Image correlation techniques have been implemented in order to get automatically the photo-coordinates  $(x, y)$  of each image of the reference points. Several levelling rods (four in our example) have been placed near the object in order to provide several regularly spaced reference points. With a few distance measurements in the object space it is easy to preview the approximated photo-coordinates of the reference points in the image and get automatically their exact object co-ordinates.

#### 4.1 Image correlation

The cross correlation method has been used. The sampled radiometric values of a (target) image with dimensions  $(m \times n)$  of a reference point belong to a random variable  $T$ . The sampling of the radiometric values of a fraction of the image with equal dimensions  $(m \times n)$  in the search window, where it is intended to find a reference point, belongs to a random variable  $S$ . The fraction  $(m \times n)$  scans the search window whose size has been previously defined. The value of the correlation ( $\rho$ ) can be found from the following formula that has been written in this convenient form, from an algorithmic point of view:

$$r = \frac{\sum g_t g_s - N \bar{g}_t \bar{g}_s}{\sqrt{(\sum g_t^2 - N \bar{g}_t^2)(\sum g_s^2 - N \bar{g}_s^2)}}, \quad \text{eq.(4)}$$

with:

- $N=m \times n$  number of pixels of the target image or of the corresponding fraction of the search window;  
 $g_t, g_s$  grey scale values of the target image and of the corresponding fraction, respectively;  
 $\bar{g}_t, \bar{g}_s$  average of the grey scale values of the target image and of the corresponding fraction, respectively.

The target image has been compared with fractions of the search window looking for the location  $(i, j)$  of the highest correlation  $\rho$ . These pairs of values  $(i, j)$  have been transformed into pairs of photo-coordinates  $(x, y)$ , what has been accomplished by an affine bi-dimensional transformation. Figure 1 shows a part of an image with the search windows (squares) and the found

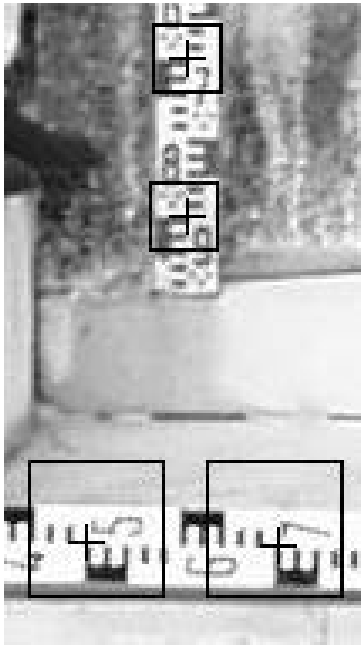


Figure 1 - Enlarged image of levelling rods, search windows (squares) and recognised targets. (crosses).

reference points (with a cross). A minimum correlation (0.4) was set, for an image to be considered as a reference point.

#### 4.2 Robust estimation

Because the minimum correlation criteria is not enough to discard locations which have been wrongly assumed as being those of reference points, some additional method has to be implemented in order to provide the automatic reading with a more acute "critical sense". Robust methods show ability to detect contaminated data because they are less affected by those erroneous observations when compared to the conventional least squares method. Out of the several robust methods available the robustified least squares approach has been used. Instead of minimising  $v^T P v$ , with  $P=D^{-1}$  and  $v=A \hat{x}-l$ , one minimises a function of  $v$ , namely its normalisation  $w$ , with

$$w_i = \frac{v_i}{s_i \sqrt{r_i}}$$

and

$$r_i = (I - A(A^T P A) A^T P)_{ii}. \quad \text{Eq.(5)}$$

The solution  $\hat{x}$  is iteratively computed, with the diagonal of  $P$  taking values, [Berberan, 1995]:

$$p_{ii} = \begin{cases} 1/s_i^2 & \text{if } w_i \leq 3.29 \\ 1/w_i^2 & \text{if } w_i > 3.29. \end{cases}$$

The value of  $\sigma_i$  is (sometimes much) smaller than 1 thus, in practical terms, the weight  $p_{ii}$  of the information carried by  $l_i$  is downgraded in accordance with a statistical test.

## 5 RESAMPLING

After the recognition of object referenced points it is possible to carry out a self-calibrating space resection which determines the exterior and interior camera parameters. It is now possible to reconstruct an image which is free of the distortion, introduced by the imaging system when the sensors were sensitised, and rectified, of the perspective effect due to the lack of parallelism between the image plane and the object plane surface. The corrected image is obtained, by using the colinearity equations and determining, in the pixels of the original image, the radiometric values for the pixels of the new image. Because the numerical images are discrete, the location of their pixels is done by a pair of integer values  $(i, j)$ . But the figures obtained from the referred colinearity equations are real numbers and this implies a process of interpolation to find out the correct  $(i, j)$  pair of integers. The nearest neighbour method of interpolation has been used for the sake of computing speed.

## 6 CASE STUDIES

The software has been loaded in a portable computer (Pentium at 100 MHz) and some experiments have been carried out. The images where downloaded to the computer, geometrically corrected and analyzed in situ. In order to quantify what might be understood by the concept of flatness, table I shows the effect, in the object space and in centimeters, of offsetting the supposed flatness, by a quantity DZ.

### 6.1 Laboratory case

A laboratory test has been carried out in order to assess empirically the expected accuracy of the method. A set of targets has been placed at regular intervals (figure 2) in a metallic structure. A vector drawing of those targets has been made with CAD software and a digital image has been taken with the photographic camera. The processed digital image (figure 3) has been superimposed to the vector drawing. An enlarged area of the superimposed images is shown in figure 4. The comparison, all over the complete overlapped images, has shown that there is no target in the corrected raster image that diverges more than half a pixel from its corresponding vector drawing target. Graphics in figures 5A) and 5B) represent

TABLE I

Effect in the object space and in centimeters of offsetting the reference plane by DZ

Focal Distance		c= 9,2 mm						c= 15 mm						c= 24 mm					
		DZ (cm)						DZ (cm)						DZ (cm)					
		1	2	3	4	5	6	1	2	3	4	5	6	1	2	3	4	5	6
RADIAL (mm)	0,5																		
	1																		
	1,5																		
	2					1,1	1,3												
	2,5				1,1	1,4	1,6							1,0					
	3				1,3	1,6	2,0							1,0	1,2				
	3,5			1,1	1,5	1,9	2,3							1,2	1,4				
	4			1,3	1,7	2,2	2,6				1,1	1,3	1,6						1,0
	4,5			1,5	2,0	2,4	2,9				1,2	1,5	1,8						1,1
	5		1,1	1,6	2,2	2,7	3,3			1,0	1,3	1,7	2,0					1,0	1,3
5,5		1,2	1,8	2,4	3,0	3,6			1,1	1,5	1,8	2,2					1,1	1,4	

distortions that have been determined in order to correct the image in figure 2.

6.2 Vectorised façade

Figure 6 contains another image gathered with the above-mentioned digital camera. After the previously referred automatic processing has been carried out, figure 7 has been produced. A heads up vectorising of the important architectonic features has taken place producing an image which is shown in figure 8. Image in figure 6 shows clearly the effects of the perspective - the object parallel lines become convergent lines in the image - and those of the deformation - the roof straight line in the object become a curved line in the image. Figure 7 is corrected of both effects.

7 CONCLUSION

Stereoscopic photogrammetry is considered as a reliable method to vectorize 3D objects. Nevertheless the photogrammetric stereoscopic method needs specialised and skilled operators as well as expensive hardware and software. On the other hand many buildings have what might be considered, to a certain extent, as flat facades. Taking advantage of that fact, it was possible to develop an easy to use, monoscopic photogrammetric software. Which allows an inexpensive methodology for the preparation of images of flat facades that can be vectorized at an acceptable accuracy (half pixel) by people without photogrammetric skills.

Setting up the control, taking a few measurements and getting the imagery may take five to fifteen minutes with a crew of two, depending on access and size of building. The semi-automatic (some tuning parameters, approximated camera position, etc. have to be inputted) image processing may take 10 to 30 minutes per image depending in image resolution and computer processing speed. No sub-pixel methods have been implemented and, accordingly, the accuracy that might be expected was achieved: half pixel.

The negative effect of the relief that exists in the so-called flat facade can be minimised with the use of an angle lens as narrow as possible.

8 REFERENCES

Berberan, A. 1992 - "Outlier Detection and Heterogeneous Observables - a Simulation Case Study", Australian Journal of Geodesy, Photogrammetry and Surveying, June 1992.

Berberan, A. 1995 - "Multiple Outlier Detection: a Real Case Study", Survey Review, Vol 33 n-255, January 1995.

Kraus, K. 1993 - "Photogrammetry", Dummler, 4<sup>th</sup> Edition, Bonn.

Mikhail, E. 1976 - "Observations and Least Squares" - IEP A Dun Donnelley Publisher, New York.



Figure 2 - Original image of a test target area



Figure 3 - Rectified image of the test target area

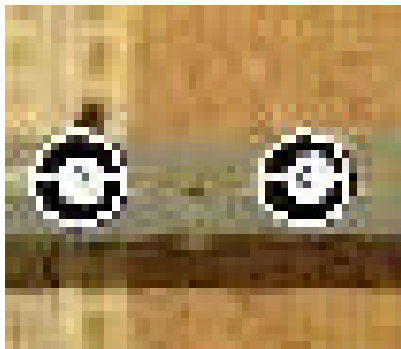


Figure 4 - Overlapping of vector drawing of targets and rectified raster image of the test area

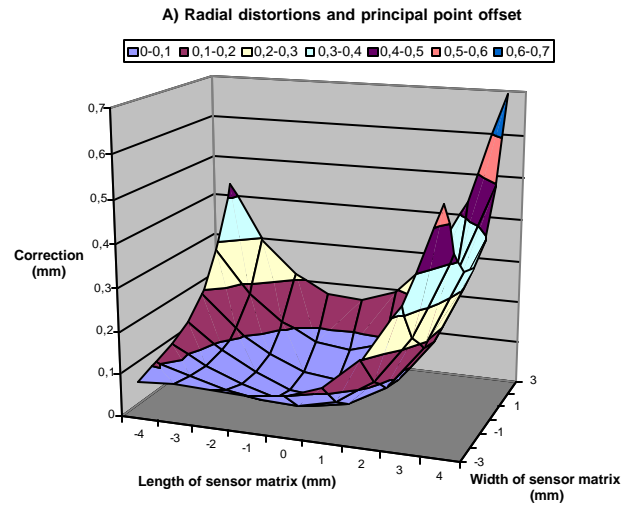


Figure 5 – Lens calibration , A), B) and C)

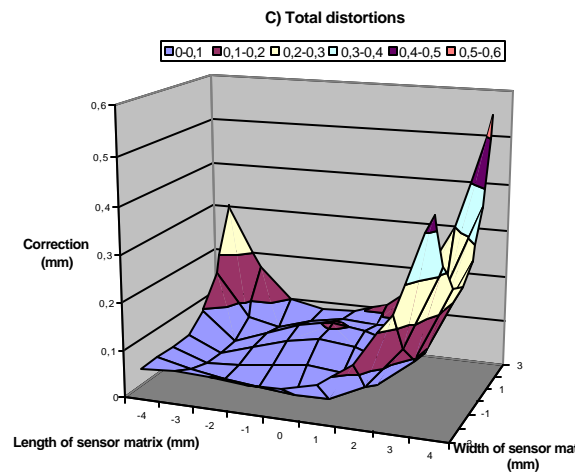
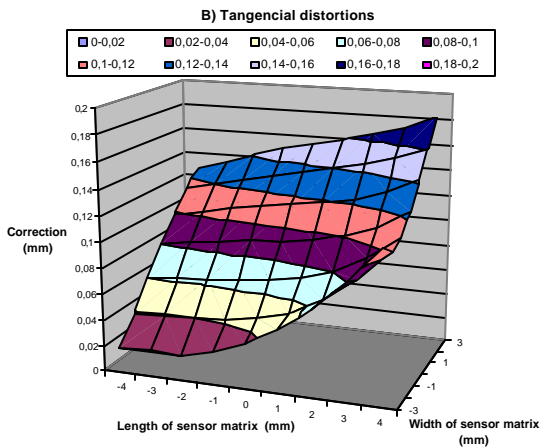






Figure 6 - Original image of the "flat" facade of a building. Effects of lens distortions and perspective are evident



Figure 7 – Rectified image

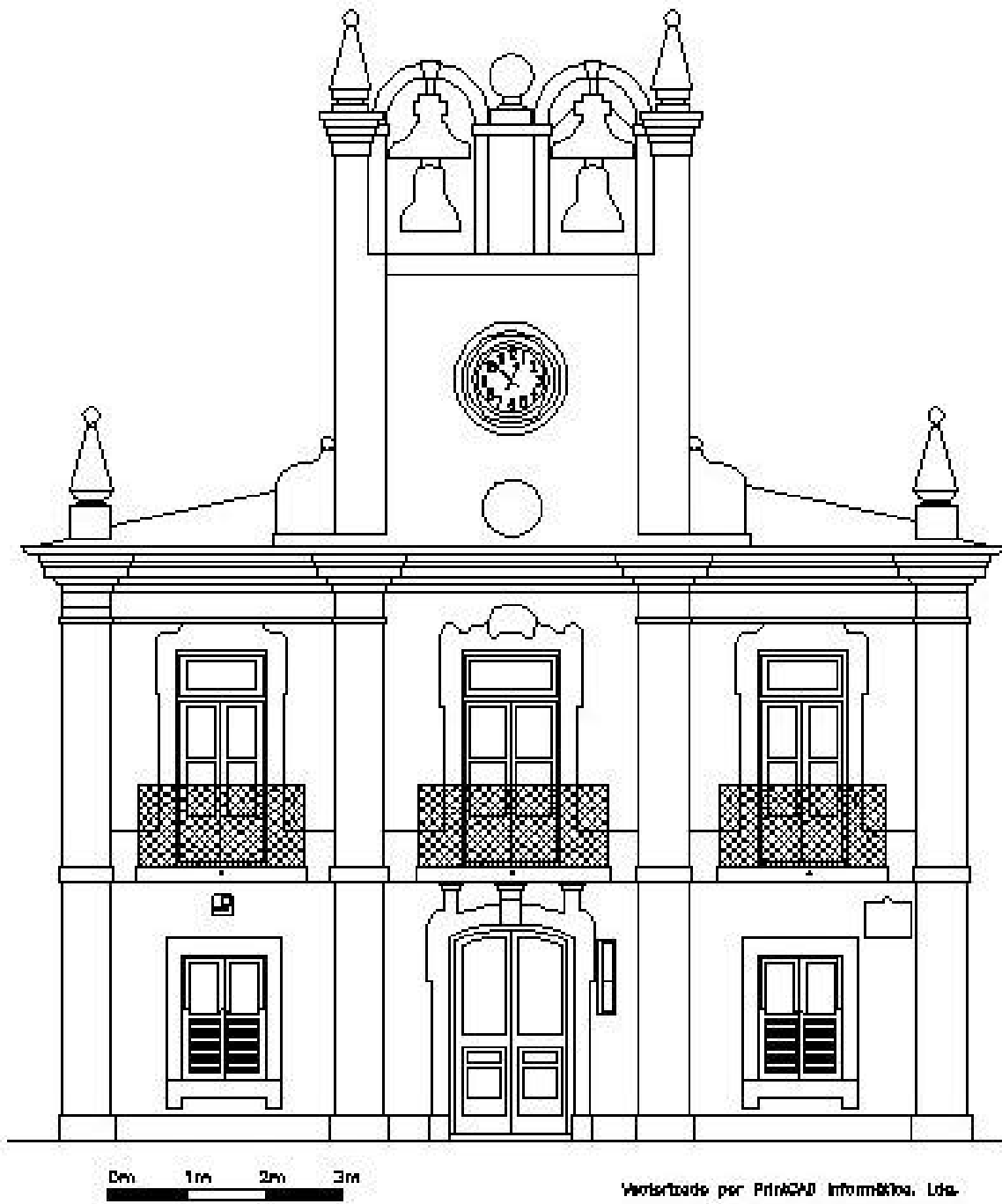


Figure 8 - Result of heads up vectorisation of rectified raster image



